Applied Mathematics 2022, 12(1): 8-16
DOI: 10.5923/j.am.20221201.02

Source-to-Sink Distribution in a Feasible Autorhythmic Volume Conduction System

Nzerem Francis Egenti*, Ukamaka Cynthia Orumie

Department of Mathematics and Statistics, University of Port Harcourt, Nigeria

Abstract Sources and sinks are phenomena of interest. Biological systems have their share of the inherent benefits derivable from them. One of such systems is the Autorhythmic Volume Conduction System (AVCS). Autorhythmicity is typical of electrically active cells that demonstrate rhythmic activity without being driven by external stimulation. It is a unique attribute of cardiac cells. Here, specialized nodal cells act as sources and sinks, with the conduction pathways maintaining the integrity of ionic flow. The edge-nodal system is a network. Feasible network flow of ionic current is often achieved by the synergy between edge-nodal appurtenances. A veritable way of analyzing network systems is the mathematical graph theory. Therefore, this was done here. Much as the AVCS has its idiosyncrasy in terms of current flow through edge-nodal structures, the analysis of electrical flow as evinced by source and sink phenomena is a clue to a better understanding of the conduction system of the heart.

Keywords Bioelectric, Graph theory, Network, Impulse, Action potential, Maximize

1. Introduction

Bioelectric phenomena predate all artificial forms of electricity. In bioelectricity endogenous electrically mediated signalling regulate cell, tissue, and organ-level modelling and behaviour. Cells and tissues of all types, in the main, use ion fluxes to communicate electrically. Bioelectric phenomena are usually described by volume conduction models. Such models describe the topology and conductivity of tissues wherein electric current flows and also the current sources in the tissue. The heart is typical of an autorhythmic volume conduction system, and it is therefore being considered here. It is here named *autorhythmic volume conduction system* (AVCS). Autorhytmicity is a unique attribute of cardiac muscle cells. The cells can generate an autonomous action potential (AP) to an enormous degree.

The passage of ionic current across the membrane of active excitable cells induces sources and sinks. In the AVCS the nodal structures, which include the sinoatrial node, atria, atrioventricular nodes (AVN), His bundles, Purkinje's fibres act as electric sources and sinks. The heart is a site for the transmission of autonomous and automatic AP. The propagation of such APs is contingent on the efficient conduction of electrical current from an excited cell to an abutting quiescent cell. *Sources* and *sinks* are created when cells give charge to abutting quiescent cells. Almost every cell in the AVCS acts as a source and a sink. The source-sink balance is an essential issue in the cardiac system. In this regard, Unudurthi *et al*. [1] depicted the pivotal role of the sinoatrial node (SAN) in the integrity of cardiac source-sink balance.

Nikolaidou *et al*. [2] showed the elegant source-sink relationships that reside in the SAN region. The consummation of the conduction system presupposes the generating of the quantity of current that would be sufficient for the local sink. This is one possible way of avoiding source-sink mismatch which is largely implicated in the deleterious cardiac events. The choice of the term *feasible* in the caption of this work implies a **mismatch-free** dipole. In this regard, Boyle and Vigmond [3], Kleber and Rudy [4] stressed safety needs and therefore the quantification of the source-sink balance.

The question of how specialized cells prosecute, nay, control the conduction system given their susceptibilities requires great attention. For instance, how does the relatively small SAN cope with the electrical exigencies of the much larger atrial tissue? Such a source-sink mismatch is also seen in the Purkinje fiber–ventricular junction where a small Purkinje fiber (source) is coupled to a large mass of ventricular tissue (sink). How do the Purkinje cells satisfy the ventricular mass to cope with a source-sink mismatch? To be quite succinct, one may read what Joyner and Capelle [5] say as regards the earlier question, and see Morley *et al*. [6] for the latter question. We are yet to define the conduction network or, if you like, pathway: This is sequentially made up of the SAN, the atrioventricular node (AVN), and the His-Purkinje system. The anatomy of each

* Corresponding author:
frankjournals@yahoo.com (Nzerem Francis Egenti)
Received: Feb. 8, 2022; Accepted: Mar. 7, 2022; Published: Mar. 28, 2022
Published online at http://journal.sapub.org/am

of the above, which is not within the scope of this work, may be found in numerous Anatomy and Physiology works of literature including Monfredi *et al.* [7] and Kurian *et al.* [8]. Cardiac myocytes are connected end to end by intercalated disks. Adjacent to the discs is the gap junctions. Of physiological and electrical importance are the low resistance gap junctions. These junctions allow APs to spread from one myocyte to the next. They decisively determine how much depolarizing current passes from excited to quiescent regions of the network. Thus, they determine the speed and safety of the conduction process [9]. Gap junctions are known sites for electrical coupling between cells. Woodbury and Crill [10] supplied a treatise on electrical potential at the gap junction between two contiguous cells way back in 1970. Writing in contemporaneous times with the former, Heppner and Plonsey [11] produced a seminal work on the electrical interaction of cardiac cells. In real cardiac tissue, however electrical conduction takes place in both the intracellular and extracellular space in cardiac tissue, wherein there are variations in conductance and anisotropic ratios. Heppner and Plonsey [11] considered the intracellular and extracellular media as passive volume conductors of longitudinal resistances.

At present, mathematical treatment of the cardiac source-sink process is sparse in literature. A detailed understanding and application of graph theory [12,13,14] seem invaluable in the study of the AVCS. This work took this reasoning into account; it presents a mathematical approach to the understanding of the AVCS mechanism which is anchored on cell-to-cell source-sink electro-physiological flow. The issue of cell-to-cell flow here was treated as a network problem (see Rubido *et al.* [15,16], Wang and Lai [17], and Ahuja *et al.* [18]).

2. Graph Theoretics of the Source-Sink Network

Let **G** = (*V, E*) be a directed graph (digraph), where *V* and *E* are the node (vertex) set and segment (edge) set respectively. Let $N = N(s, t)$ be a network, with two distinct vertices- a source *s* and a sink *t*, together with a non-negative real-valued function *c* defined on its arc set *A*. The vertex *s* corresponds to a production centre, or in the present case the impulse generating node, and the vertex *t* to a consumer, or the adjoining impulse receiving node. The function *c* is the *capacity function* of *N* and its value on a segment *l is the capacity* of *l*. The capacity of a segment *may* be seen as the maximum rate at which a substance can be transported through it.

An (*s, t*)-*flow* in *N* is a real-valued function *f* defined on a set *S* such that

$$f^{+}(v) = f^{-}(v) \text{ for all } v \in I, \tag{1}$$

where *v* represents a generalized vertex, *I* is the set of all intermediate vertices. Condition (1) is known as the *conservation condition*. A *feasible* flow must satisfy, in addition, the capacity constraint:

$$0 \le f(l) \le c(l) \text{ for all } l \in A \tag{2}$$

The upper bound in condition (2) imposes the natural restriction that the rate of flow along a segment cannot exceed the capacity of the segment.

Definition 1. [13] *Let f be a feasible flow in a network N. A source-to-sink segment in a graph* ***G*** *is an f-augmenting path P such that for each* $l \in E(P)$*:*

(a) $f(l) < c(l)$ *when P follows l in the forward direction.*

(b) $f(l) > 0$ *when P follows l in the backward direction.* (3)

Suppose $\tau(l) = c(l) - f(l)$ when *l* is forward on *P*, and let $\tau(l) = f(l)$ when *l* is backward on *P*. The *tolerance* of *P* is

$$\text{Tol}(P) = \min_{l \in E(P)} \tau(l). \tag{4}$$

Definition 2: *A directed graph G = (V, E) is* ***strongly connected*** *if and only if, for each pair of nodes* $u, v \in V$*, there exists a path from u to v.*

2.1. Graph Metrics

Graph metrics reveal the diverse characteristic of a defined network. Some salient ones are as follows:

2.1.1. Integration Metric

This estimates the relative ease with which cell regions communicate. If v_i and v_j are two adjoining nodes then the *Shortest Path Length* (SPL) between them is the shortest path that reaches v_j *beginning* from v_i. It is the shortest number of edges between v_i and v_j; for a weighed graph SPL is the sum of all the edge weights in the shortest path between v_i and v_j, calculated as

$$s_{ij} = \sum_{b_{a,u} \in G_{i \Leftrightarrow j}} b_{a,u} \tag{5}$$

where $G_{i \Leftrightarrow j}$ is the shortest path between v_i and v_j.

In measuring functional integration global efficiency is the choice metric.

Definition 3 (**Bryan *et al*.** [**19**]) Let P_n denote the path on vertices $v_1, v_2, \ldots, v_n$ with edges v_1v_2, v_2v_2 …, $v_{n-1}v_n$. The distance $d(v_i, v_j)$ between distinct vertices v_i and v_j is $|i - j|$. Hence the efficiency between different vertices v_i and v_j is

$$E(v_j, v_j) = \frac{1}{d(v_j, v_j)} = \frac{1}{|i - j|}.$$

The global efficiency of the graph is calculated as

$$E_{Glob}(P_n) = \frac{2}{n.(n-1)} \left(\sum_{t=1}^{n-1} \frac{n-t}{t} \right) \tag{6}$$

2.1.2. Segregation Metric

This measures the presence of clusters or modules within the network. Modularity is the degree to which a network may be partitioned into prominently delineated and non-overlapping groups. We may not bother much about the

intricacies of this metric since the network in this study is not as complex as to require its use.

2.1.3. Measure of Centrality

Degree centrality is calculated by counting the neighbours of each vertex. It is given by

$$c_D(v_k) = \frac{\deg(v_k)}{n-1} \tag{7}$$

with $v_k \in V$, V the set of nodes, $n = |V|$ and $\deg(v_k)$ the degree of node v_k.

Closeness centrality is calculated by summing distances from a vertex to each other. It is encoded as

$$c_D(v_k) = \frac{\deg(v_k)}{n-1} \tag{8}$$

with $v_k \in V$, $n = |V|$ and $dis(v_i, v_j)$ the distance from node v_i to node v_j.

For a vertex v, betweenness centrality is defined as [20]

$$c_B(v) = \sum_{s \neq v \neq t} \frac{\sigma_{st}(v)}{\sigma_{st}}, \tag{9}$$

where σ_{st} is the total number of shortest paths from node and $\sigma_{st}(v)$ is the number of those paths that pass through v (not where v is an end point).

Describing betweenness centrality of a node v in proportionality to the number of occurrences of itself on all geodesics of a graph, the evaluation is [21]:

$$c_B(i) = \frac{2\sum\sum \frac{g_{jk}(i)}{g_{jk}}}{(n-1)(n-2)}, \tag{10}$$

where g_{jk} is the number of geodesics from node x_j to node v_k, $g_{jk}(i)$ the number of geodesics from x_j to v_k containing v_i; the double sum is evaluated on all pairs (j,k) such that $j \neq i \neq k$ and $j < k$.

2.1.4. Measure of Resilience

This is a metric of the vulnerability of the network as regards functional integration.

2.2. Impulse Transmission on the Conduction Network

The graph **G** = (V, E) here is treated as analogous to an electric network. Kirchhoff's flow network is ideal in the treatment of minimal cost in transportation, including biological steady-state systems. We assume that the flow network obeys Ohm's law. Thus,

$$L_{ij}^{(s\,t)} = (V_i^{(s\,t)} - V_j^{(s\,t)}) = R_{ij}\, f_{ij}^{(s\,t)}. \tag{11}$$

In the above equation, the left-hand side $L_{ij}^{(s\,t)} = V_i^{(s\,t)} - V_j^{(s\,t)}$ represents voltage drop across the segment ($i \rightarrow j$) connecting nodes at i and j, with a source situated at node s and a sink situated at node t. The segment ($i \rightarrow j$) has a resistance R_{ij} against the flux f_{ij} which is determined by the conductance of the segment l. By conservation condition (11), the net flow at any node in the network must vanish. Therefore,

$$\sum_{i,j=1}^{N} f_{ij}^{(s\,t)} = 0, \tag{12}$$

except at the source s and the sink t. The net flow at node i is governed by the Kirchhoff law:

$$\sum_{j=1}^{N} f_{ij}^{(s\,t)} = \sum_{j=1}^{N} W_{ij} L_{ij}^{(s\,t)}, \tag{13}$$

where the bandwidth W_{ij} of the segment ij is inversely proportional to the resistance R_{ij}. $W_{ij} \approx 1/R_{ij}$ is the matrix representation of the network arrangement, (see [22] in which such arrangement was treated).

2.2.1. Constructing the Adjacency Matrix of the AVCS

Definition 4. The *adjacency matrix* of a directed graph ***G*** is the number of edges that issue from vertex v_i and go into vertex v_j. Thus, if $D = (d_{ij})$ is the adjacency matrix of ***G***, then

$$d_{ij} = \text{number of arcs that issue from vertex } v_i \text{ and go into vertex } v_j. \tag{14}$$

The adjacency matrix of the AVCS is constructed using **Fig. 1(b)** or equation (**14**) as (see Nzerem and Ugorji [24])

$$A_{ij} = \begin{array}{c} \begin{matrix} v_1 & v_2 & v_3 & v_4 & v_5 & v_6 \end{matrix} \\ \begin{pmatrix} 0 & 0 & 0 & 0 & 0 & 0 \\ 3 & 0 & 0 & 0 & 0 & 0 \\ 0 & 1 & 0 & 0 & 0 & 0 \\ 0 & 0 & 1 & 0 & 0 & 0 \\ 0 & 0 & 1 & 0 & 0 & 0 \\ 0 & 0 & 0 & 1 & 0 & 0 \end{pmatrix} \begin{matrix} v_1 \\ v_2 \\ v_3 \\ v_4 \\ v_5 \\ v_6 \end{matrix} \end{array} \tag{15}$$

In **(**15**)** above v_i on the row indicates the initial node of an arc e_j while each v_j on the column indicates the terminal vertex of the arc. From (14) we have

$$A_{ij} = \begin{cases} 1, & \text{if node } i \text{ connects node } j \\ 0, & \text{if } i \text{ and } j \text{ are disjoint} \end{cases} \tag{16}$$

Each of the nodes represents a part of the ACVS, to wit- Sinoatrial node (SAN), v_1, atrioventricular node (AVN), v_2, the bundle of HIS bifurcation point, v_3, the left bundle of HIS branch v_5, and the right bundle of HIS branch v_6. It is instructive to note that

$$d^+(v_1) \cong 3 \text{ and } d^-(v_1) = 0 \tag{17}$$

For any isolated node v_k,

$$d^+(v_k) = 0 \text{ and } d^-(v_8) = 0. \tag{18}$$

For a networked system, the total flow at any node obeys Kirchhoff conservation law:

$$F_i = \sum_{j=1}^{N} A_{ij} f_{ij} = \sum_{j=1}^{N} A_{ij} W_{ij} L_{ij}^{(st)} = 0 \tag{19}$$

where A is the adjacency matrix of the network. Another

defining component of the network is the Laplacian matrix, **M**, of the fundamental network, which is obtainable from **MV** = **F**, whose elements are given by

$$M_{ij} = \begin{cases} \sum_{i=1}^{N} A_{ij} / R_{ij}, & i = j \\ -A_{ij} / R_{ij} & i \neq j. \end{cases} \tag{20}$$

Such a matrix was detailed in [24].

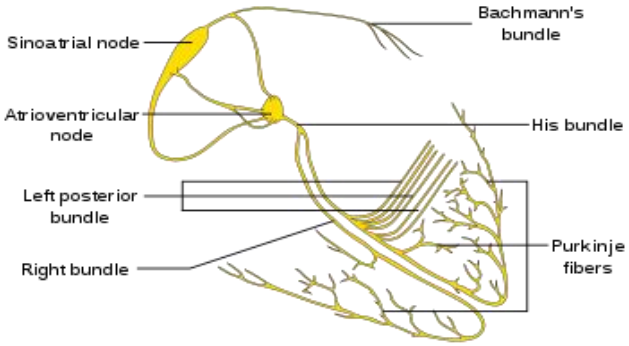

Figure 1(a). Electrical conduction system of the heart [23]

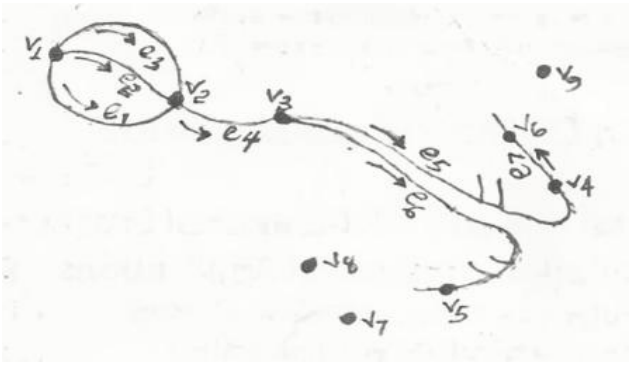

Figure 1(b). Node-edge schematic of the CCS [24]

3. Ionic Flow and Action Potential

Like biological fluid-structure interaction problems [25], the cell-to-cell flow consists of the cardiac cellular structures and the ionic substances in current. However, unlike the Eulerian formulation that characterizes fully developed fluid flow, the present flow is amenable to Kirchhoff's laws. The treatment of general cardiac APs is somewhat herculean due to variations in the constitutive ions and APs of the various cardiac myocytes. It would seem rather plausible to treat conduction in cell-to-cell segmentations, thereby accommodating their idiosyncratic APs (see Qu *et al*. [26]). In the AVCS, the electrical impulse is generated in the SAN, which spreads quickly through the atria to the atrioventricular node (AVN). (Note that the SAN is electrically coupled to the atria). The impulse travels from the AVN to the His-Purkinje system. Eventually, the Purkinje fibres transmit the impulse to the ventricular muscles at numerous discrete locations. The problem of source-to-sink distribution involves triggering an AP in a quiescent cell by an abutting active cardiac cell. The architecture of a cardiac strand, with its many individual cells of irregular shapes, is a mathematical task. Here each cell is assumed cylindrical and non-tapering.

3.1. Bidomain Electrical Flow

Bidomain structure defines a model of the heart tissue comprising two interpenetrating domains representing cardiac cells and the surrounding space, the intracellular and the extracellular domain [27,28]. The continuous topology of the intracellular space enhances ion travel from the inside of one cell to another via gap junctions without getting into the extracellular space, nor would ion travelling in the extracellular region require entry to the cell. Both spaces have electrical autonomous properties, therefore they form an anisotropic medium.

Let the associated internal and external potentials of the domains be Φ_i and Φ_o. Then the transmembrane potential is $V = \Phi_i - \Phi_o$. The current associated with the internal and external potentials are $-\sigma_i \nabla \Phi_i = i_i$ and $-\sigma_o \nabla \Phi_o = i_o$ respectively. By Kirchhoff law

$$\nabla.(\sigma_i \nabla \Phi_i) = B_m I_m \tag{21}$$

$$\nabla.\ (\sigma_i \nabla \Phi_i + \sigma_o \nabla \Phi_o\ ) = 0, \tag{22}$$

where I_m represents the current through the cell membrane dividing the two regions, B_m is the ratio of the surface area and the cell volume. The transmembrane current has the form [29]

$$I_m = C_m \frac{\partial V}{\partial t} + I_{ion} \tag{23}$$

Current flows through the boundary of extracellular space, but this is not so at boundary of intracellular space [30]. The boundary conditions for the bidomain model is of the form

$$\begin{aligned} &\mathbf{n}.(\sigma_i \nabla \Phi_i) = 0, \\ &\mathbf{n}.(\sigma_o \nabla \Phi_o) = I(t,x) \quad on \quad \partial\Omega \end{aligned} \tag{24}$$

where Ω is the cardiac domain, ***n*** is the outer unit normal vector to the boundary $\partial\Omega$. Since the flow of net current must be zero, we have

$$\int_{\partial\Omega} I(t,x) dS = 0 \tag{25}$$

Thus, charge accumulation does not exist in a feasible flow since any entering current must be exiting.

3.2. Potential Field and Current in the Gap Region

Here we consider the potential field in the inter-gap region between two abutting cells. Two abutted identical cylindrical fibres of radius r_o, one assumed active and the other assumed inactive, are separated by a distance δ.

Define the potential field $\epsilon(r, z)$ in the region, $0 < z < \delta$; $0 \leq r \leq r_o$. It is assumed that: the fibres are draped with non-excitable membranes, with specific resistance R_d (Ω-cm^2); the end-cap resistances R_d are entirely passive and do not depend on voltage; the flow of current depends only

on the voltage drop across the gap. In the specified region, the potential ϵ will satisfy Laplace's equation $\nabla^2\varepsilon(r,z)=0$. With the cylinder assumed axisymmetric we have

$$\frac{1}{r}\frac{\partial}{\partial r}\left(r\frac{\partial\varepsilon}{\partial r}\right)+\frac{\partial^2\varepsilon}{\partial z^2}=0 \tag{26}$$

With the membranes assumed thin and situated at $z = 0$ and $z = \delta$ the associated boundary conditions are [10]:

(i) $\dfrac{\varepsilon(r,0^+)-\varepsilon_a}{R_d}=\sigma\left.\dfrac{\partial\varepsilon}{\partial z}\right|_{z=0^+}$,

(ii) $\dfrac{\varepsilon(r,\delta^-)}{R_d}=-\sigma\left.\dfrac{\partial\varepsilon}{\partial z}\right|_{z=\delta^-,}$,

(iii) ε finite at $r = 0$,

(iv) $\varepsilon = 0$ at $r = r_o$.

With the rest of the present section emphasizing [10], conditions (iii) and (iv) are imposed to have a solution of equation (24) is in the form

$$\varepsilon(r,z)=\sum_{n=1}^{\infty}J_0(k_nr)[A_n\cosh(k_nz)+B_n\sinh(k_nz)], \tag{27}$$

where k_n are the roots of $J_o(k, r) = 0$. Applying boundary conditions (*i*) and (*ii*) gives

$$\sum_{n=1}^{\infty}A_nJ_0(k_nr)-\varepsilon_a=R_d\sum_{n=1}^{\infty}k_nB_n(k_nr),$$

and

$$\sum_{n=1}^{\infty}J_0(k_nr)[A_n\cosh(k_n\delta)+B_n\sinh(k_n\delta)]$$
$$=R_d\sigma\sum_{n=1}^{\infty}J_0(k_nr)k_n[A_n\cosh(k_n\delta)+B_n\sinh(k_n\delta)].$$

The coefficients A_n and B_n by multiplying both sides of the above two equations by $rJ_0(k_mr)$, integrating with respect to r over $[0,r_0]$ and applying the orthogonality property of the Bessel functions. Substitute the resulting expressions into equation (25) and get

$$\varepsilon(r,z)=\varepsilon_a$$
$$\sum_{n=1}^{\infty}\frac{2J_0(k_nr)}{(d_n+\sigma R_dk_n)k_nr_0J_1(k_nr_0)}.[d_n\cosh(k_nz)-\sinh(k_nz)], \tag{28}$$

where

$$d_n=[\sigma R_dk_n+\tanh(k_n\delta)]/[1+\sigma R_dk_n\tanh(k_n\delta)].$$

The gap region accommodates current density $-\sigma\nabla\varepsilon$, with ε given by equation (28) above. Three notable currents come to play. They are the currents crossing the active and quiescent disc surfaces and the current across the cylindrical wall at $r = r_0$ $(0 < z < \delta)$. Denote these currents by *IA*, I_Q, and I_W respectively. The total current flowing into the gap from *IA* is

$$I_A=-2r\sigma\int_0^{r_0}r\left.\frac{\partial\varepsilon}{\partial z}\right|_{z=0}dr.$$

The current flowing into the quiescent cell is

$$I_Q=-2r\sigma\int_0^{r_0}r\left.\frac{\partial\varepsilon}{\partial z}\right|_{z=\delta}dr.$$

The residual current, I_W, across the cylindrical gap boundary is

$$I_W=-2r\sigma\int_0^{r_0}r\left.\frac{\partial\varepsilon}{\partial r}\right|_{r=r_0}dz.$$

Substitute equation (26) into the above three equations and interchange the order of integration to get

$$I_A=4\pi\sigma r_0\varepsilon_a\sum_{n=1}^{\infty}\frac{1}{e_n}, \tag{29}$$

$$I_Q=-4\pi\sigma r_0\varepsilon_a\sum_{n=1}^{\infty}\frac{1}{e_n}[d_n\sinh(k_n\delta)-\cosh(k_n\delta)], \tag{30}$$

$$I_W=4\pi\sigma r_0\varepsilon_a\sum_{n=1}^{\infty}\frac{1}{e_n}[d_n\sinh(k_n\delta)-\cosh(k_n\delta)+1], \tag{31}$$

where

$$e_n=(d_n+\sigma R_dk_n)k_nr_0,$$
$$dn=\frac{\sigma R_dk_n+\tanh(k_n\delta)}{1+\sigma R_dk_n+\tanh(k_n\delta)}.$$

3.3. Source-Sink Analysis

Source-sink interaction, which is achieved through excitation, is a sine qua non to the proper functioning of the SAN and other cardiac cells. The excitability of a cell can be expressed loosely as the ease with which a response could be prompted. It is often described as the least possible current necessary to depolarize the membrane to the threshold potential [31]. Electric sources of bioelectric origin are generated by the passage of current across the membrane of active (excitable) cells. How depolarizing 'source' current generated by the SAN drives depolarization and activation of the contiguous atrial tissue (current 'sink') remains uncertain. Bioelectric sources can refer to surface/volume distributions of two types of source elements, that is, the *monopole* and/or *dipole*. The dipole is a combination of a source and sink of equal strength. In the conduction system, the self-excitatory SAN is the leading source of action potential. (Note: From Fig. 1(b) or using (17) we have)

$$d^+(v_1)\cong 3 \text{ and } d^-(v_1)=0.$$

The zero indegree indicates the inherent self-excitatory property Of the SAN. The SAN and the AVN constitute a dipole. In a similar mode, the AVN and the HIS bundle constitute a dipole. In effect, every activated sink becomes a source. Suppose *f* is a feasible flow and [*S, T*] is a source/sink cut, then the net flow out of *S* and net flow into *T* equal *val*(*f*). Assume flow from SAN to HIS bundle is feasible (as in a

physiological flow), we have

$$f^{+}(U)-f^{-}(U)=\sum_{v\in}\left[f^{+}(U)-f^{-}(U)\right] \quad (32)$$

with U as a set of nodes in the section of the network being considered [13].

Assume a cylindrical conducting medium wherein a point source (the SAN) is located. In this regard, we may require the equation of the field of the point source inside the medium, with co-ordinates (ρ,ϕ,z). Thus, the potential of a unit source located at some point (ρ_0,ϕ_0,z_0) inside the tube, which is bounded above and below by the planes $z = -L$ and $z = L$ and on the sides by the cylinder $\rho = a$ *may* be sought. As L approaches infinity the field of the point source inside the conducting cylinder is given by [32]

$$V(\rho,\varphi,z)=\sum_{n=0}^{\infty}\sum_{r=0}^{\infty}A_{nr}J_n(k_{nr}\rho)\cos\left(n(\varphi-\varphi_0)\right)e^{-k_{nr}|z-z_0|}$$
$$A_{nr}=\frac{2(2-\delta_{n0})}{a^2}\frac{J_n(k_{nr}\rho_0)}{k_{nr}\left[J_{n+1}(k_{nr}a)\right]^2}, \quad (33)$$

The modified equation of SAN membrane current is given by [23]

$$I=\mathrm{C_M}\frac{dV}{dt}+\frac{1}{C_M}(i_{Ca,L}+i_{Ca,T}+i_{Kr}+i_{Ks}+i_{Na}[\delta_{Na}(\mathrm{A})]+i_{to}+$$
$$\{gf_{Na}[\delta_{Na}(A)]\,y(V-E_{Na})+f_K y(V-E_K)\}+i_{sus}), \quad (34)$$

$$\delta_{Na(A)}=\begin{cases}1, & \text{if } Na\in A\\ 0, & \text{otherwise}\end{cases} \quad (35)$$

where:

A be the intra-cellular region consisting of the SAN

$i_{Ca,L}$, i_{CaT} are L- and T-type Ca^{2+} currents;

$i_{K,r}$, $i_{K,s}$ are rapid and slow delayed rectifying K^+ currents;

i_f (the funny current) is the hyperpolarization-activated current given by

$\{gf_{Na}[\delta_{Na}(\mathrm{A})]\;\; y(V-E_{Na})+f_K y(V-E_K)\}$;

Na^+ is the sodium ion;

i_{st} is the sustained current;

i_{to} is the transient outward current.

C_m is the membrane capacitance.

The canonical form of the equation of transmembrane current is (23)

$$I=C_m\frac{\partial V}{\partial t}+I_{ion}$$

Considering equations (29) and **(**23**)** and taking the SAN as the active cell (source), the transiting current, which would drive depolarization and activation of the contiguous cell is

$$4\pi\sigma r_0\varepsilon_a\sum_{n=1}^{\infty}\frac{1}{e_n}=C_m\frac{\partial V}{\partial t}+I_{ion}, \quad (36)$$

where I_{ion} is the total ionic currents exiting the SAN.

Equation (36) holds well for the SAN as a source, which recruits excitation through the atria to the adjoining AVN cells. The time-dependent membrane voltage may be furnished by the non-linear two-dimensional Fitzhugh-Nagumo equations, which describe the behaviour of an excitable cell. The equations read:

$$\frac{\partial V^*}{\partial t}=\frac{1}{\varepsilon}\left(V^*-\frac{V^{*2}}{3}-W\right)\equiv\eta(V^*,W) \quad (37)$$

$$\frac{\partial W}{\partial t}=\varepsilon\left(V^*-\gamma W-\beta\right)\equiv\eta(V^*,W), \quad (38)$$

where V^* encodes the membrane voltage, W is a quantity associated with the recovery of the cell after it fires, ϵ, γ, and β are non-negative dimensionless parameters. Equation (38) may be seen as the current equation; the capacitive charging term, proportional to dV^*/dt, on the left and the nonlinear channel currents on the right. The form of equation (37) shows that the recovery of the cell is denoted as a gate opening equation with voltage-dependent rates. The amplitude of ϵ corresponding to the inverse of a time constant determines the rate with which W changes relative to V. The analysis of the system of equations (37) and (38 is by the method of phase plane, which may be found in [33].

3.4. Node-Edge Capacity and Maximal Flow

A source-sink mismatch is a deleterious liability to numerous impulsive systems. Some biological systems manage to overcome source-sink imbroglio through some anatomical topology. Bartos *et al*. [34] noted that the ability of SAN to overcome the source-sink mismatch to activate the surrounding atrial myocardium stem from the distinctive anatomy of gap junction proteins. The capacity of an edge c_{ij} may be expressed as the bandwidth of the edge, being the maximum flux that the edge can deliver devoid of cramming or damage. Thus, the capacity bandwidth of an edge is inversely proportional to the edge resistance, we write

$$c_{ij}=\lambda/R_{ij}, \quad (39)$$

where λ is a capacity parameter.

Assume for convenience first that the AVCS network has n nodes that consist of a single source SAN and a single sink AVN. We tag the source node 1 and the sink node n. Let c_{ij} denote the capacity of arc (i,j). For a flow in this network, let x_{ij} denote the quantity flowing from node i to node j along an arc (i,j). Then x_{ij} must satisfy

$$0\le x_{ij}\le c_{ij}, \quad i,j=1,2,...,n. \quad (40)$$

One finds that

$$\sum_{i=1}^{n}x_{ik}-\sum_{j=1}^{n}x_{jk}=0, \quad k=2,3,...,n-1 \quad (41)$$

A formulation of the maximal flow problem is

$$\text{Maximize } f=\sum_{k=1}^{n}x_{\mathbf{1}k} \quad (42)$$

Subject to

$$\sum_{i=1}^{n} x_{ik} - \sum_{j=1}^{n} x_{jk} = 0, \qquad k = 2, 3, ..., n-1 \tag{43}$$

$$0 \le x_{ij} \le c_{ij}, \quad i, j = 1, 2, ..., n.$$

The maximal flow problem furnishes a linear programming problem, which may be solved using some programming methods (see Kolman and Beck [35]).

The cost implication of the flow may be required. The work by Hung and Chien [36] may be employed to find such cost. In this regard, let **E** be the path from vertex *u* to vertex *v* through edges e_j, j=1, 2, ..., (r+1), and vertices u_j, j=1, 2, ..., h. Thus,

$$\mathbf{E} = [u, e_1, u_1, e_2, u_2, \ldots e_h, u_h, e_{h+1}, v] \tag{44}$$

The cost of passing a unit of service of kind l (in this case, current), l = 1, 2,…,w, through the path **P**, encoded by $Je_l(P)$, is given by

$$J_l(P) = \sum_{j=1}^{r+1} Je_l(e_j) + \sum_{j=1}^{r} Jv_l(u_j, e_j, e_{j+1}) \tag{45}$$

where $Je_l(e)$ is the edge cost function, Jv_l the node switch cost function. An issue of great importance is how to maximize flow at the least cost. This however is not within the purview of the present work. If $Je_l(e) = \infty$, it is illegal to pass service on a path e. If $Jv_i = \infty$, it is an illegal edge to pass a service from e_i through v_i to edge e_j ($i \neq j$). In the AVCS segment, where $d^+(v_1) \cong 3$ and $d^-(v_1) = 0$, the edge cost of SAN-AVN transmission involves maintaining three (3) transmission lines to ensure that the individual (and by extension the total) capacity c_{ij} of the edges is not compromised.

3.4.1. AVCS Global Efficiency

The question of AVCS global efficiency may be difficult to furnish from the standard equation (6). This arises from the fact that for each of the expressed nodes v_k, other than the SAN, $d^-(v_k) = 1$. It is of note that, by **Definition 2,** the AVCS graph is *not strongly* connected.

The centrality concept measures the importance of nodes in a graph network. Here the graph is the G_{AVCS} whose nodes are not interconnected. Centrality may be from the standpoint of the impact of a node on other nodes. Following [37], let v^* be the node with the highest degree centrality in G. Let $X := (Y, Z)$ be the $|Y|$ node connected graph that maximizes the quantity (with y^* being the node with highest degree centrality in X):

$$H = \sum_{j=1}^{|Y|} \left[C_D(y^*) - C_D(y_j) \right], \tag{46}$$

where $C_D(.)$ is the centrality degree of a given node. Therefore, the *degree centralization* of the graph G is

$$C_D(G) = \frac{\sum_{i=1}^{|V|} \left[C_D(v^*) - C_D(v_i) \right]}{H} \tag{47}$$

H is maximized when graph X contains one central node to which all other nodes are connected. For any graph G,

$$C_D(G) = \frac{\sum_{i=1}^{|V|} \left[C_D(v^*) - C_D(v_i) \right]}{|V|^2 - 3|V| + 2} \tag{48}$$

Degree centrality is the most widely used measure of centrality. Since it measures the number of direct neighbours of a node, it explains the importance of the node in a given network. In the brain network, it measures the influence of a brain region on adjacent brain regions [35]. In the AVCS network analysis, the degree centrality of a cardiac nodal cell shall measure the influence of a nodal cell on other nodal cells. In the AVCS we have,

SAN:

$$d^+(v_1) = 0 \quad \text{and} \quad d^-(v_1) = 3,$$

AVN:

$$d^+(v_2) = 3 \quad \text{and} \quad d^-(v_2) = 1. \tag{49}$$

HIS Bundle:

$$d^+(v_3) = 1 \quad \text{and} \quad d^-(v_3) = 2. \tag{50}$$

It may matter to consider the system based on weighted degree centrality on the out-degree of the neighbours. Thus, the Katz centrality measure

$$x_i = \frac{1}{\lambda} \sum_j A_{ij} x_j + \beta \tag{51}$$

holds, A is the adjacency matrix of the graph G with eigenvalues *lambda*, β is a constant initial weight given to each vertex so that vertices with zero in-degree (or out-degree) are included in calculations (see Gera [38]).

4. Summary and Conclusions

Sources and sinks are typical of flow phenomena. A source is a place/point of inception of flow whereas a sink is a place/point of accumulation of flow. Thus, a sink is a negative source. In nature, there is no presupposition of all-time source and sink of equal strength (dipole). In the bioelectric flow considered, sources and sink mismatch exist without prejudice to the physiological vivacity of the immediate and remote cells involved in the mechanism of flow. The bioelectric conductor considered here is the AVCS. As a rule, the driver of cell-to-cell AP is ionic current. Although the heart is both functionally and anatomically complex, humans, and perhaps animated life with cardiac structures, are compensated by the *non-strongly connected* nature of its electric flow network. A strongly connected network system is more or less a culprit in the event of deleterious cascading failures. In the event of SAN failure, the AVN is a known surrogate pacemaker, which can initiate the firing of AP to the contiguous cell, the His bundle. In the absence of autonomic nervous stimulation, the rate of ventricular contraction is set at 40–60 bpm by the AVN. It is

instructive to note that the serial surrogate responsibility of the AVCS cells is largely compensatory and as well averting.

Source and sink system is a network issue. This work employed the benefits of graph theory in analyzing the AVCS. An essential requirement of a network is the efficiency of the edge and nodal structures. Global efficiency is a measure of cumulative effect of the edge-nodal system, especially concerning strongly a connected weighted graph. Given the nature of connectedness of the AVCS, cardiac efficiency is often defined in terms of the mechanics of the heart rather than the electrical system (see for instance [39]). Some interesting points are worthy of note/ emphasis:

(i). The AVCS consists of pairs of sources and sinks of unequal strength.

(ii). Source and sink mismatch of the AVCS is anatomical, but it may be implicated in pathophysiological conditions. (However, in an anatomical state, it would not be an independent marker of a cardiac event.)

(iii). The *non-strongly connected* nature of the AVCS is an ethereal blessing, as it slows down the rate of cascading failures following any segmental/nodal disorder. This accounts for the relative enduring life of the critical organs in the event of mild to serious AVCS disorder.

(iv). The cost of achieving maximal flow is not of necessity an economic one; it requires maintaining the node-edge vivacity.

Since autochthonous electrical excitation resides in the SAN, which is the source of AP transmission, and since the other conduction nodes are surrogate pace-makers, it is reasonable to believe that the resolution of conduction anomaly can be found by in-depth analysis of source and sink system associated with the AVCS.

ACKNOWLEDGEMENTS

The authors are grateful to the reviewers for their meaningful input that helped in the revision of this work.

REFERENCES

[1] S.D. Unudurthi, R.M. Wolf and T.J. Hund, Role of sinoatrial node architecture in maintaining a balanced source-sink relationship and synchronous cardiac pacemaking, frontiers in Physiology, Volume 5, Article 446, 2014, doi:10.3389/fphys.2014.00446.

[2] T., Nikolaidou, O.V., Aslanidi, H., Zhang, and, I.R Efimo, 2012, Structure-function relationship in the sinus and atrioventricular nodes. Pediatr. Cardiol. 33, 890–899. doi:10.1007/s00246-012-0249-0.

[3] P.M. Boyle, and E.J. Vigmond, 2010, An intuitive safety factor for cardiac propagation. *Biophys. J.* 98, L57–L59. doi:10.1016/j.bpj.2010.03.018.

[4] Kleber, A. G., and Y. Rudy, 2004, Basic mechanisms of cardiac impulse propagation and associated arrhythmias. *Physiol. Rev.* 84, 431–488, doi:10.1152/phys-rev.00025.2003.

[5] R.W. Joyner and F. J. L. van Capelle, 1986, Propagation through electrically coupled cells, How a Small SA Node Drives a Large Atrium, Biophysical Journal, Volume 50, p1157-1164.

[6] G.E Morley, S.B. Danik,, S. Bernstein, Y. Sun, G. Rosner, D.E. Gutstein, 2005, Reduced intercellular coupling leads to paradoxical propagation across the Purkinje-ventricular junction and aberrant myocardial activation, Proc. Natl. Acad. Sci. U.S.A. 102, 4126–4129.doi:10.1073/pnas.0500881102.

[7] Monfredi, O., Dobrzynski, H., Mondal, T., Boyett, M. R. and Morris, G. M., 2010, The Anatomy and Physiology of the Sinoatrial Node—A Contemporary Review. Pacing and Clinical Electrophysiology, 33: 1392–1406. doi: 10.1111/j.1540- 8159.2010.02838.x.

[8] Kurian, T., Ambrosi, C., Hucker, W., Fedorov, V. V. and Efimov, I. R., 2010, Anatomy and Electrophysiology of the Human AV Node. Pacing and Clinical Electrophysiology, 33: 754–762. doi: 10.1111/j.1540-8159.2010.02699.x.

[9] Stephan Roh, r2004, Role of gap junctions in the propagation of the cardiac action potential, Cardiovasc Res 62 (2): pp. 309-322. doi:https://doi.org/10.1016/j.cardiores.2003.11.035.

[10] J. W. Woodbury and W. E. Crill, 1970, The potential in the gap between two abutting cardiac muscle cells a closed solution, Biophysical Journal Vol. 10, pp.1076-1083.

[11] D. B. Heppner and R. Plonsey, Simulation of electrical interaction of cardiac cells, Biophysical Journal Volume 10 1970, pp. 1057-1075.

[12] J.A. Bondy and U.S.R. Murty, Graph theory, Springer, 2008.

[13] Douglas B. West, Introduction to Graph theory (second edition), Rashtriya Printers, India, 2002 https://archive.org/details/igt_westy.

[14] Keijo Ruohonen, 2013, Graph theory, [Online]. Available: http://www.flooved.com/reader/3467.

[15] Rubido N., Grebogi1 C. and Baptista, M. S. 2013, Structure and function in flow networks, EPL, 101 68001, doi: 10.1209/0295-5075/101/68001.

[16] Rubido N., Grebogi1 C. and Baptista, M. S., Understanding Information Transmission in Complex Networks, 2017 arXiv:1705.05287v1 [nlin.AO].

[17] W-X Wang. and Y-C Lai., Abnormal cascading on complex networks, PHYSICAL REVIEW E 80, 036109, 2009, pp.1- 6, DOI: 10.1103/PhysRevE.80.036109.

[18] Ahuja R. K. Magnanti T. L. and OrlinJames B.,, Network Flows: Theory, Algorithms, and Applications, Prentice Hall, NJ, 1993.

[19] E. Bryan, C. VerSchneide, J. Lind, and D. A. Narayan, Real World Graph Efficiency. [Online]. Available: *http://www.math.iit.edu › teaching › GoodModules.*

[20] L. C. Freeman, "A set of measures of centrality based on betweenness," *Sociometry*, vol. 40, pp. 35–41, 1977.

[21] Yannick Rochat, Closeness Centrality Extended To

Unconnected Graphs: The Harmonic Centrality Index.

[22] Nzerem F.E., Ugorji H.C., Cardiac Electrophysiology: The Sinoatrial Node in Focus, Mathematics Letters, 2018; 4(4): 59-66, doi: 10.11648/j.ml.20180404.11.

[23] Electrical conduction system of the heart, [Online]. Available: https://en.wikipedia.org/wiki/Electrical_conduction_system_of_the_heart.

[24] Nzerem F. E. and Ugorji H.C., 2019, Cardiac Conduction System: The graph theoretic approach, j. Math. Comput. Sci. 9 No. 3, 303-326, https://doi.org/10.28919/jmcs/4027.

[25] Nzerem F. E.and Alozie H.N., 2013, The Underlying Physiology of Arterial Pulse Wave Morphology in Spatial Domain, Appl. Appl. Math., Vol. 8, Issue 2, pp. 495 – 505.

[26] Z. Qu, G.Hu, A. Garfinkel, and J. N. Weiss, 2014, Nonlinear and Stochastic Dynamics in the Heart, Phys Rep., 543(2): 61–162. doi: 10.1016/j.physrep.2014.05.002.

[27] Sachse, F. Computational Cardiolgy: Modeling of Anatomy, Electrophysiology and Mechanics. LNCS 2966. Springer, Berlin, 2004.

[28] Keener, J.P., and Sneyd, J. Mathematical Physiology. Springer-Verlag. New York, 1998.

[29] Hodgkin, A. L. and Huxley, A. F. (1952). A quantitative description of membrane current and its application to conduction and excitation of nerve, J. Physiol. 117, 500-544.

[30] Jairo V. G, Andrus G. M., 2012, The Electrical Activity of Cardiac Tissue via Finite Element Method Adv. Studies Theor. Phys., Vol. 6, no. 20, 995 - 1003.

[31] M. Vornanen, 2020, Feeling the heat: source–sink mismatch as a mechanism underlying the failure of thermal tolerance, *J Exp Biol*, 223 (16), https://doi.org/10.1242/jeb.225680.

[32] Point current source and a conducting sphere. [Online]. Available: https://em.geosci.xyz/content/...sources.../point_current_source_and_sphere.html.

[33] Phase plane analysis, [Online]. Available: http://icwww.epfl.ch/~gerstner/SPNM/node22.html.

[34] D. C. Bartos, E. Grandi, and C. M. Ripplinger, 2015, Ion Channels in the Heart, Compr Physiol. Jul 1; 5(3): 1423–1464, doi: 10.1002/cphy.c140069.

[35] B. Kolman, R. E. Beck, Special Types of Linear Programming Problems in Elementary Linear Programming with Applications (Second Edition), 1995. [Online]. Available: https://www.sciencedirect.com/topics/computer-science/augmenting-path.

[36] H. V. Hung, and T.Q. Chien, 2020, Maximal concurent limited cost flow problems on extended multi-commodity multi-cost network, American Journal of Applied Mathematics, 8(3): 74-82.

[37] Centrality. [Online]. Available: https://en.wikipedia.org/wiki/Centrality.

[38] R. Gera, Katz Centrality for directed graphs [Online]. Available: *http://faculty.nps.edu›rgera›06-CentralitiesKatz.*

[39] J. Sörensen, H. J. Harms, J. M. Aalen, T. Baron, O.A. Smiseth, P. Frank, A. Flachskampf, 2020, Myocardial Efficiency: A Fundamental Physiological Concept on the Verge of Clinical Impact, JACC: Cardiovascular Imaging Volume 13, Issue 7, pp 1564-1576.